Gene 827 (2022) 146473

Contents lists available at ScienceDirect

Gene

journal homepage: www.elsevier.com/locate/gene

Research paper

A nuclear receptor heterodimer, CgPPAR2-CgRXR, acts as a regulator of carotenoid metabolism in *Crassostrea gigas*

Sai Wan [a], Qi Li [a,b,*], Hong Yu [a], Shikai Liu [a], Lingfeng Kong [a]

[a] Key Laboratory of Mariculture, Ministry of Education, Ocean University of China, 5 Yushan Road, Qingdao 266003, China
[b] Laboratory for Marine Fisheries Science and Food Production Processes, Qingdao National Laboratory for Marine Science and Technology, Wenhai Road, Qingdao 266237, China

ARTICLE INFO

Edited by: John Doe

Keywords:
Crassostrea gigas
Nuclear receptors
Peroxisome proliferator-activated receptor
Retinoid X receptor
Heterodimer
Carotenoid metabolism
Ligands

ABSTRACT

Nuclear receptors (NRs) are mostly ligand-activated transcription factors in animals and play essential roles in metabolism and homeostasis. The NR heterodimer composed of PPAR/RXR (peroxisome proliferator-activated receptor/retinoid X receptor) is considered a key regulator of lipid metabolism in vertebrate. However, in molluscs, how this heterodimer is involved in carotenoid metabolism remains unclear. To elucidate how this heterodimer regulates carotenoid metabolism, we identified a *PPAR* gene in *C. gigas*, designated as *CgPPAR2* (LOC105323212), and functionally characterized it using two-hybrid and reporter systems. *CgPPAR2* is a direct orthologue of vertebrate *PPARs* and the second *PPAR* gene identified in *C. gigas* genome in addition to *CgPPAR1* (LOC105317849). The results demonstrated that CgPPAR2 protein can form heterodimer with *C. gigas* RXR (CgRXR), and then regulate carotenoid metabolism by controlling carotenoid cleavage oxygenases with different carotenoid cleavage efficiencies. This regulation can be affected by retinoid ligands, i.e., carotenoid derivatives, validating a negative feedback regulation mechanism of carotenoid cleavage for retinoid production. Besides, organotins may disrupt this regulatory process through the mediation of CgPPAR2/CgRXR heterodimer. This is the first report of PPAR/RXR heterodimer regulating carotenoid metabolism in mollusks, contributing to a better understanding of the evolution and conservation of this nuclear receptor heterodimer.

1. Introduction

Nuclear receptors (NRs) are transcription factors regulating expressions of genes involved in development, homeostasis, and metabolism (Mangelsdorf et al., 1995). NRs commonly contain the conserved DNA-binding domain (DBD) and ligand-binding domain (LBD). The DBD allows NRs to bind to the *cis*-regulatory elements in the promoters of specific genes, and the LBD is responsible for dimerization, transactivation and ligand binding (Novac and Heinzel, 2004; Laudet, 2006). Ligands interacting with NRs are signaling molecules mainly including lipophilic hormone molecules such as steroid and thyroid hormones as well as organotin compounds, such as tributyltin (TBT) and triphenyltin (TPT), that can mimic hormones (Hessel et al., 2007; Diamanti-Kandarakis et al., 2009).

As dietary lipids, carotenoids are precursors of some signaling molecules, e.g., All-*trans*-RA (ATRA), 9-*cis*-RA (9CRA), and they must be cleaved and metabolically converted by intrinsic carotenoid cleavage oxygenases (BCOs) to produce retinoids, which support vitamin-A dependent signaling pathways (Hessel et al., 2007). In vertebrates, it has been established that carotenoid cleavage process is under a typical metabolic negative feedback loop. For instance, the carotenoid-15,15′-oxygenase (BCO1) is the key enzyme of carotenoid cleavage in rat and chicken, and is regulated by NRs, such as retinoic acid receptor (RAR), peroxisome proliferator-activated receptor (PPAR), retinoid X receptors (RXR) (Boulanger et al., 2003; Lobo et al., 2010a; Amengual et al., 2011). This is a useful mechanism to help organisms deal with

Abbreviations: PPAR, peroxisome proliferator activated receptor; BCO, carotenoid cleavage oxygenase; RAR, retinoic acid receptor; RXR, retinoid X receptor; TCC, total carotenoid content; EGFP, enhanced green fluorescent protein; qRT-PCR, quantitative real-time PCR; TPM, transcripts per million; DBD, DNA binding domain; LBD, ligand binding domain; FBS, fetal bovine serum; DLR, dual-luciferase reporter; DPBS, Dulbecco's phosphate buffered saline; DMSO, Dimethyl sulfoxide; TBT, tributyltin; TPT, triphenyltin; ATRA, All-*trans*-Retinoic acid; 9CRA, 9-cis- Retinoic acid; NR, nuclear receptor; Y2H, Yeast Two-Hybrid; DDO, double drop out medium; TDO, triple drop-out medium; 3′AT, 3-Amino-1,2,4-triazole; QDO, quadruple drop-out medium; NLS, nuclear localization signal.

* Corresponding author at: Key Laboratory of Mariculture, Ministry of Education, Ocean University of China, 5 Yushan Road, Qingdao 266003, China.
E-mail address: qili66@ouc.edu.cn (Q. Li).

https://doi.org/10.1016/j.gene.2022.146473
Received 29 January 2022; Received in revised form 23 March 2022; Accepted 31 March 2022
Available online 4 April 2022

fluctuations in carotenoid supply (Fitzpatrick et al., 2012).

In particular, the PPAR/RXR heterodimer has been identified as a key regulator of lipid homeostasis in vertebrates (Casals-Casas et al., 2008; Tyagi et al., 2011), including the regulation of carotenoid metabolism through the control of BCO1 (Bachmann et al., 2002; Boulanger et al., 2003; Hessel et al., 2007). Moreover, this heterodimer is modulated by natural ligands fatty acids, e.g., Arachidonic acid (ARA) and *cis*-5,8,11,14,17-Eicosapentaenoic acid (EPA), and retinoids (Xu et al., 1999; Santos et al., 2018), as well as man-made chemicals such as organotins (Capitao et al., 2018). In vertebrates, there are three paralogs of *PPAR* (α, β and γ) (Capitao et al., 2018)) and the PPAR/RXR heterodimer is permissive, which means that it can be activated by PPAR and/or RXR ligands (Harada et al., 2015; Ouadah-Boussouf and Babin, 2016)).

The fact that *PPAR* is present in deuterostomes and mollusks, while *RXR* is present in most metazoans (Vogeler et al., 2017; Capitao et al., 2018; Santos et al., 2018; Fonseca et al., 2020; Capitao et al., 2021), suggests that the PPAR/RXR heterodimer may play similar roles in these species. Depending on the species, there are one or two *PPAR* genes (*PPAR1* amd *PPAR2*) in molluscs (Vogeler et al., 2014; Vogeler et al., 2017), of which *PPAR2* has been demonstrated to be an orthologue of vertebrate *PPARs* (Kaur et al., 2015). However, in invertebrates, limited studies on the PPAR/RXR heterodimer have mainly focused on their influence by environmental disruptors (Lyssimachou et al., 2009; Pascoal et al., 2013; Capitao et al., 2021). Furthermore, recent phylogenetic analyses of carotenoid cleavage oxygenases (CCOs) in metazoans have revealed the existence of a BCO2-like clade (BCOL) in lancelet, nematode, and molluscs, which is ancient in origin and independent of BCO1 and BCO2 (Poliakov et al., 2017). Whereas it remains to be resolved whether these BCOL enzymes are controlled by the PPAR/RXR heterodimer in invertebrate species.

Mollusk, like other animals, acquire carotenoids from their diet, i.e., various algae filtered from seawater, which are abundant in carotenoids (Maoka, 2011; Takaichi, 2011). Actually, carotenoid metabolism in mollusks, have been reported in relation to NRs. For instance, RAR and RXR were demonstrated to be involved in the accumulation of total carotenoid content (TCC) of polymorphic *Chlamys nobilis* under different light cycles (Tan et al., 2021).

The Pacific oyster, *Crassostrea gigas*, is one of the most ecologically and economically important species. Study of the metabolic mechanism of carotenoids in this species is beneficial for the possible utilization of carotenoids in *C. gigas*. Recently, identification of *C. gigas* NRs (Vogeler et al., 2014), and then the functional characterization of *CgRXR*, *CgRAR* and *CgPPAR* has been reported (Vogeler et al., 2017; Huang et al., 2020; Jin et al., 2021), but the described *CgPPAR* gene (LOC105317849, designated as *CgPPAR1*) was reported as the only *PPAR* gene in *C. gigas* and is not a direct orthologue of vertebrate PPARs, as shown by phylogenetic analysis (Capitao et al., 2021). Notably, our previous study reported that dietary beta-carotene supplement led to down-regulation of *BCOL* genes in *C. gigas* (designated as *CgBCOL* genes), thus raising the hypothesis that there is a negative feedback regulation of *CgBCOL* genes involving NRs in *C. gigas* (Wan et al., 2022).

In this work, among the NRs reported in our previous study, we identified a *PPAR* gene (LOC105323212, designated as *CgPPAR2*) in *C. gigas*, a direct orthologue of vertebrate *PPAR* genes that can heterodimerize with *CgRXR*, and regulate carotenoid metabolism by controlling *CgBCOL* genes and interacting with ligands. To our knowledge, this work is the first to investigate the relationship between the PPAR/RXR heterodimer and carotenoid metabolism in mollusks and contributes to understanding of the regulation of carotenoid metabolism and the knowledge of its evolutionary conservation.

2. Materials and methods

2.1. Oyster collection, ligand injection and tissue sampling

One-year old Pacific oysters were collected from Rushan, Shandong province, China (36.4°N, 121.3°E). The shell height and total weight were 100.41 ± 14.01 mm and 85.14 ± 13.72 g, respectively. All oysters were acclimated in aerated artificial seawater at 14 ℃ for at least 10 days and fed with *Chlorella vulgaris*, with 300 million algal cells per oyster per day for satiation (Kuhn et al., 2013) before experiments were undertaken.

For the ligand injection experiment, a total of 24 oysters were divided into 2 tanks. To test the response of oysters to the typical organotin (e.g., TPT), the adductor of oysters in the experiment group was injected with TPT dissolved in DMSO (3 μl per dose, 1.5 μg/μl). The group injected with DMSO was used as the control group. Injections were performed every two days, for a total of five injections, referring to the dose used by Giraud-Billoud et al. (2019). At end of the experiment, digestive gland (Dgl) were dissected from the survived oysters ($n \geq 4$) of every group, immediately frozen in liquid nitrogen and stored at −80 ℃ for subsequent total RNA extraction, reverse transcription, PCR and quantitative real-time PCR (qRT-PCR) analyses.

2.2. Identification, sequence and phylogenetic analyses of nuclear receptor and carotenoid cleavage oxygenase genes

Given that *C. gigas* NRs have been identified by Vogeler et al. (2014), we used the identified full-length NR protein sequences as well as their DBDs and LBDs to perform BLASTp search against protein sequences derived from the latest Pacific oyster representative genome (GenBank accession No. GCA_902806645.1). Then the domains of obtained protein sequences were annotated with the Conserved Domain Database (CDD) of NCBI (Marchler-Bauer et al., 2011). Proteins with LBD and/or DBD were identified as NRs.

Phylogenetic analyses were performed using the amino acid sequences of *C. gigas* NRs and their metazoan homologues retrieved from NCBI. A total of 348 NR protein sequences (File S1) were aligned using MAFFT v7.471 (Katoh et al., 2002) by the method of L-INS-I method. An unrooted phylogenetic tree was constructed by the Maximum-Likelihood (ML) algorithm using IQ-Tree 1.4.3 (Minh et al., 2013), in which topological stability was evaluated by 1000 bootstrapping replicates.

For all five *CgBCOL* genes, we classified them into three groups based on the sequence similarities analyzed in our previous work (Wan et al., 2022): *CgBCOLa* (LOC105341121), *CgBCOLb* (LOC105321989, LOC117690758), and *CgBCOLc* (LOC105348216, LOC117684251). Then, protein and promoter sequence similarities were calculated for all five *CgBCOL* genes. Signal peptides of CgBCOL proteins were predicted by SignalP 5.0 (Almagro Armenteros et al., 2019), followed by conserved domain annotation using CDD of NCBI. Similar to the phylogenetic analyses of NRs, a total of 203 BCO protein sequences (File S2) were used for phylogenetic analyses of CgBCOL proteins. The phylogenetic tree of BCOs was rooted by archaeal oxygenase proteins as an outgroup.

2.3. RNA extraction and expression analyses

Total RNA was extracted from the digestive glands of oysters using RNA-easy Isolation Reagent (Vazyme, Nanjing, China) following the manufacturer's protocol. Subsequently, cDNA was synthesized from total RNA using HiScript III RT SuperMix for qPCR (+gDNA wiper) (Vazyme) according to the manufacturer's instructions.

To validate the expressions and sequences of newly identified NRs, cDNA from digestive glands was used for PCR amplification of NR gene regions containing LBD and/or DBD followed by TA cloning and sanger sequencing. The primers used are listed in Table S1.

In order to compare gene expression of *CgPPAR2* between the ligand-injected and control group, gene specific primers were designed using Primer-Blast at NCBI (Ye et al., 2012) (Table S1). According to the manufacturer's protocol, qRT-PCR was performed on a Roche Light-Cycler 480 Real-time PCR System (Roche, Switzerland) using EvaGreen 2x qPCR MasterMix-No Dye (ABM) with Enlongation Factor as the internal control (Renault et al., 2011). Two technical replicates were tested for each biological replicate ($n \geq 4$). Real-time PCR Miner (https://www.miner.ewindup.info/) (Zhao and Fernald, 2005) was used to calculated PCR efficiencies, optimal cycle threshold (Ct) values and relative gene expression levels normalized to Enlongation Factor. Student's *t*-test was performed for the comparison between two groups. $P < 0.05$ was considered statistically significant.

To analyze the expression profile of interested genes in different tissues, including adductor muscle (Amu), mantle (Man), digestive gland (Dgl), female gonad (Fgo), male gonad (Mgo), gill (Gil), haemolymph (Hem) and labial palps (Lpa), the raw RNAseq data released by Zhang et. al. (2012) and Xu et. al. (2021) were downloaded from EBI (ftp://ftp.sra.ebi.ac.uk, Run Accession: SRR334212, SRR334213, SRR334214, SRR334215, SRR334216, SRR334217, SRR334218, SRR334219, SRR334220), then trimmed with fastp v0.20.1 (Chen et al., 2018). The resulting clean data were mapped to the latest oyster reference genome, followed by transcript assembly conducted by StringTie v2.1.2 (Pertea et al., 2015). The transcripts per million (TPM) values were calculated for all expressed genes using IsoformSwitchAnalyzeR v1.13.05 (Vitting-Seerup and Sandelin, 2019).

2.4. Analysis of the CgBCOL function in beta-carotene cleavage

With the signal peptides removed, the CDS of *CgBCOLa, CgBCOLb, CgBCOLc* were subcloned into the pET-28a (+) to form fusion expression plasmids, using two appropriate restriction enzymes and T4 DNA ligase. Restriction enzymes sites and primers are listed in Table S1. The beta-carotene-producing plasmid, pAC-BETAipi (Cunningham and Gantt, 2005; Cunningham and Gantt, 2007), were purchased from Addgene (https://www.addgene.org/, #53277).

Each expression plasmid and beta-carotene-producing plasmid were mixed together to reach the same concentration in the same solution and used for co-transformation into *E. coli* JM109 (DE3). The three colonies obtained with both kinds of plasmids (experiment groups) were cultured to OD600 ≈ 0.6 and then induced by IPTG (2 mM) for 16 h at 20 ℃ in the dark. Expressions of CgBCOL in *E. coli* JM109(DE3) were detected by SDS-PAGE on 7.5% gels stained with Coomassie Brilliant Blue R250. The relative densities of bacteria (C) were estimated by a linear relationship calculated from OD600 values and gradient dilutions of the cultures. Bacterial cells were collected from 200 ml cultures by centrifugation, and the pellets were extracted with 4 ml of acetone by shaking at 200 rpm/min for 3 h in a dark incubator at 20 °C. After centrifuging and filtering through 0.22 μm filters, the absorbance of supernatants was determined at the wavelength of 480 nm using a spectrophotometer (UNICO UV-2800A, China). Meanwhile, single colonies containing beta-carotene-producing plasmids and empty pET28a (+) were used as positive control, and those containing only empty pET28a (+) were used as negative control. The beta-carotene cleavage efficiencies (E) of CgBCOL protein were calculated by the following equation:

$$E = \left(1 - \frac{\frac{A_e}{C_e} - \frac{A_n}{C_n}}{\frac{A_p}{C_p} - \frac{A_n}{C_n}}\right) \times 100\%$$

where A_e, A_p and A_n are absorption values at 480 nm for the experiment, positive control groups and negative control groups, and the C_e, C_p and C_n are relative bacterial densities of these groups, respectively. The experiment was repeated three times and the cleavage efficiency were presented as mean ± SD. Furthermore, a one-way ANOVA analysis was performed, in which $P < 0.05$ was considered statistically significant.

2.5. Cell culture and dual-luciferase reporter assays

HEK293T cells were cultured in complete media containing 90% DMEM (Solarbio, China), 10% fetal bovine serum (FBS) (HyClone, Logan, UT) and 1% penicillin/streptomycin (pen/strep) at 37 ℃ and 5% CO_2 in a humidified atmosphere. Then cells were transferred to 24-well plates (Corning, USA) under the same culture conditions. When cell confluence reached 60% ~ 70%, transient transfection of appropriate combinations of plasmids was performed with Lipofectamine 3000 (Invitrogen) and OptiMEM.

Two dual-luciferase reporter (DLR) systems including pcDNA3.1/pGL3-Basic and pBind/pACT (mammalian two-hybrid system) were used in the present study, and details on the use of the plasmids and ligand compounds are listed in Table S2. All Primers used are listed in Table S1, and the constructed plasmids were verified by sanger sequencing.

In the pcDNA3.1/pGL3-Basic system, the full-length CDS of *CgPPAR2* and *CgRXR* were inserted into pcDNA3.1 (expression vector) to form the fusion plasmids pcDNA3.1-CgPPAR2 and pcDNA3.1-CgRXR. Similarly, three representative promoter sequences of *CgBCOL* gene were cloned into pGL3-Basic (reporter vector). A combination of 400 ng expression vector (fused or empty), 100 ng reporter vector (fused or empty) and 50 ng control vector pRL-TK was used for transfection. Twenty-four hours after transfection, cells were cultured with fresh complete medium, and after another 24 h, luminescent activities of Firefly Luciferase (fused or empty pGL3-Basic) and Renilla Luciferase (pRL-TK) were measured using the Dual-Luciferase Reporter Assay System (Promega, USA) on a Synergy H1 Microplate Reader (Biotek).

In the pBind/pACT system, the LBD and Hinge domains of CgPPAR2 and CgRXR were subcloned into the pBind vector to construct fusion plasmid pBind-CgPPAR2 LBD and pBind-CgRXR LBD. The produced fusion proteins containing the DBD of the GAL4 transcription factor from yeast, i.e., CgPPAR2 LBD-GAL4 DBD, CgRXR LBD-GAL4 DBD. Furthermore, the LBD and Hinge domains of CgRXR were cloned into the pACT vector to form pACT-CgRXR LBD plasmid and produce a fusion protein containing the viral VP16 (CgRXR LBD-VP16).

In order to test the protein–protein interaction between CgPPAR2 LBD and CgRXR LBD, cells transfected with 150 ng pBind-CgPPAR2 LBD, 150 ng pACT-CgRXR LBD and 200 ng pGL4.31 were used as the experiment group. Cells transfected with plasmids without either or neither of the LBDs were used as negative controls. No ligand was added in this experiment.

For single LBD transfections, HEK293T cells were transfected with 150 ng pBind-CgPPAR2 LBD or pBind-CgRXR LBD, 150 ng empty pACT and 200 ng pGL4.31. For analysis of the CgPPAR2/CgRXR heterodimer, cells were transfected with 150 ng pBind-CgPPAR2 LBD, 150 ng pACT-CgRXR and 200 ng pGL4.31. Five hours after transfection, cells were washed with Dulbecco's phosphate buffered saline (DPBS) and cultured with phenol red-free DMEM supplemented with 10% dextran-coated charcoal-treated serum, 1% pen/strep and ligands. All ligands were dissolved in sterile Dimethyl sulfoxide (DMSO). The final concentration of DMSO per well was<0.1% (v/v) and the concentrations of ligands were as follows: ATRA (0 μM, 1 μM, 2 μM, 3 μM), 9CRA (0 μM, 1 μM, 2 μM, 3 μM), TBT (0 μM, 0.1 μM, 0.2 μM, 0.3 μM), TPT (0 μM, 0.1 μM, 0.2 μM, 0.3 μM), ARA (0 μM, 100 μM, 200 μM, 300 μM), EPA (0 μM, 100 μM, 200 μM, 300 μM). The following day, luciferase activities were tested as described above. Technique replicates for each test condition and the entire experiment were performed at least twice.

Transactivation results of both systems are calculated by normalizing the ratio between Firefly luciferase and Renilla luciferase luminescent activities to the empty or solvent control (normalized fold induction). Data are presented as the mean ± SD of normalized fold induction and were analyzed by one-way ANOVA, where $P < 0.05$ is considered statistically significant.

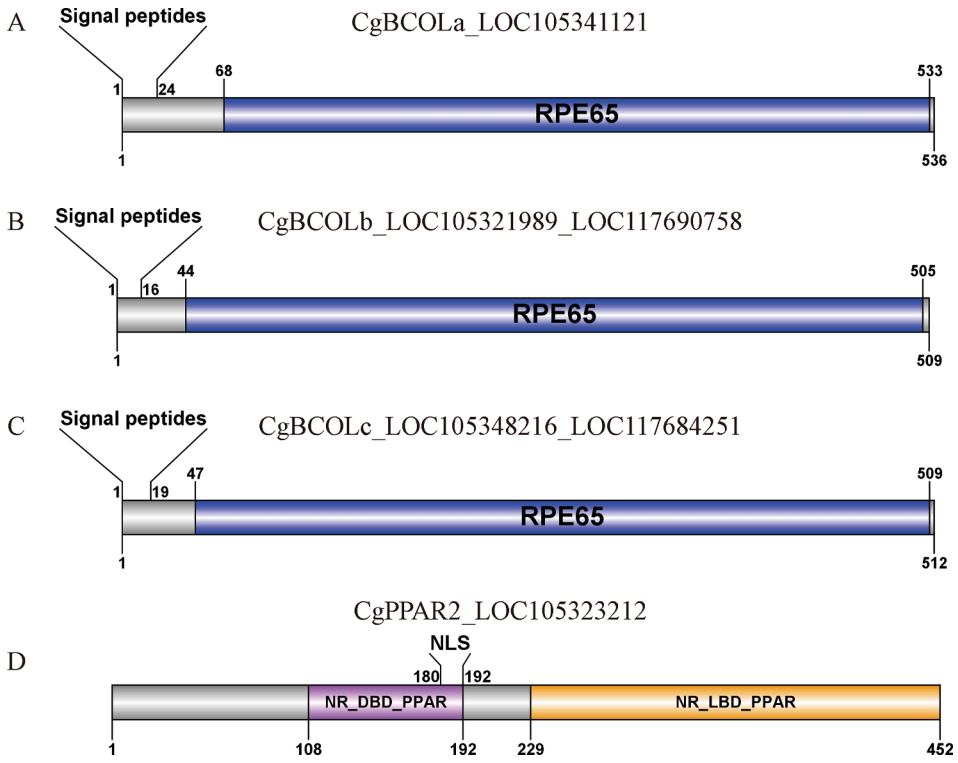

Fig. 1. Schematic diagrams of CgBCOL (A, B, and C) and CgPPAR2 (D) proteins.

2.6. Yeast two-hybrid assay

To construct fusion plasmids, the LBDs of CgPPAR2 and CgRXR were subcloned into PGBKT7 and PGADT7 respectively, to generate PGBKT7-PPAR-LGD and PGADT7-RXR-LGD plasmids. The Primers for plasmid construction are listed in Table S1.

To test the protein–protein interaction between CgPPAR2 and CgRXR, the yeast strain Yeast Two-Hybrid (Y2H) Gold was co-transferred with fusion plasmids according to the manufacturer's instructions, and then grew on SD/-Leu/-Trp double drop out medium (DDO) for three days. Then the interaction was detected based on the ability of the yeast transformants to grow on SD-Trp-Leu-His triple drop-out medium (TDO) with 5 mM 3-Amino-1,2,4-triazole (3′AT) and SD/-Ade/-His/-Leu/-Trp quadruple drop-out medium (QDO).

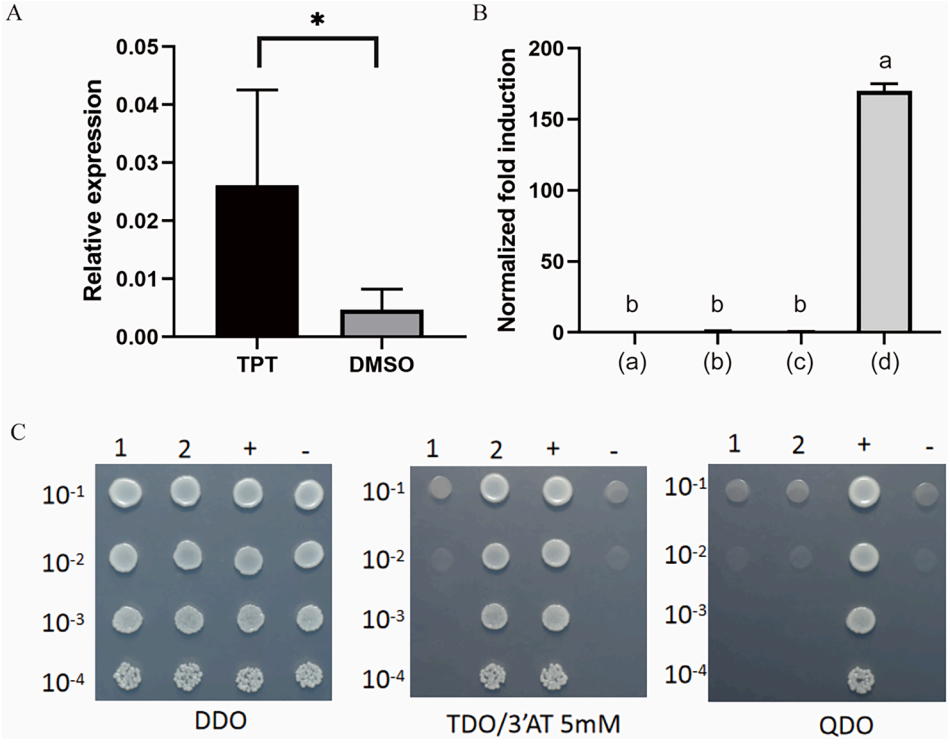

Fig. 2. (A) Response of CgPPAR2 in the digestive glands after TPT injection. Student's *t*-test was performed for the comparison between two groups. $^*P < 0.05$ was considered statistically significant. (B) Analysis of the protein–protein interaction between CgPPAR2-LBD and CgRXR-LBD using a mammalian two-hybrid assay in HEK293T cells. The results are expressed as normalized fold induction (mean ± SD). A one-way ANOVA analysis was performed and columns marked with different letters were significantly different ($P < 0.05$). (a) pBind-CgPPAR2, empty pACT, pGL4.31; (b) empty pBind, pACT-CgRXR, pGL4.31; (c) pBind-CgRXR, empty pACT, pGL4.31; (d) pBind-CgPPAR, pACT-CgRXR, pGL4.31. (C) Yeast two-hybrid assay for interactions between CgPPAR2 LBD and CgRXR LBD proteins. (1) Y2H yeast strain with PGBKT7-PPAR-LG and PGADT7. (2) Y2H yeast strain with PGBKT7-PPAR-LG and PGADT7-RXR-LG. (+)Y2H yeast strain with pGBKT7-53 and pGADT7-T, positive control. (-)Y2H yeast strain with pGBKT7-lam and pGADT7-T, negative control. DDO, double drop-out medium. TDO/3′AT mM, SD-Trp-Leu-His triple drop-out medium with 5 mM 3′AT. QDO, SD/-Ade/-His/-Leu/-Trp quadruple drop-out medium. 3′AT, 3-Amino-1,2,4-triazole.

2.7. Subcellular localization of CgPPAR2

The nuclear localization signal (NLS) sequence of CgPPAR2 was identified using the online tool SeqNLS (Lin et al., 2012). Primers with appropriate restriction enzyme sites (Table S1) were designed for subcloning the full-length coding sequence (CDS) of *CgPPAR2* into the *pEGFP-N1* plasmid to generate an in-frame fusion (pEGFP-CgPPAR2) with green fluorescent protein (GFP). When the HEK293T cells had grown to 60% influence, pEGFP-CgPPAR2 were transferred into cells with Lipofectamine 3000 (Invitrogen), to produce the fusion protein, CgPPAR2-GFP. After 24 h, cells were stained with Hoechst 33,342 (Solarbio) for 30 min so that the nuclei showed blue fluorescence. Fluorescent signal was observed with a Leica TCS SP8 confocal microscope.

3. Results

3.1. Identification, expression pattern, sequence and phylogenetic analyses of NRs and CgBCOL genes

Regarding nuclear receptor genes, four new NRs were identified based on BLASTp search and domain annotation. Sequences of their conserved domain regions were verified by sanger sequencing (File S3). Correspondences between the NRs identified by Vogeler et al. (2014) and this study were listed in the Table S3, where notably, we named LOC105323212 as *CgPPAR2*. The NLS and conserved domains of CgPPAR2 protein, i.e., NR_DBD_PPAR (accession number: cd06965) and NR_LBD_PPAR (accession number: cd06932), are shown in Fig. 1D. Previously published RNA-seq data of Zhang et al. (2012) and Xu et al. (2021) were used to analyze gene expression patterns in tissues of healthy adult oysters. The results revealed that nuclear receptor CgPPAR2 and CgRXR are ubiquitously expressed in adult *C. gigas* (Fig. S1). In addition, to investigate the response of CgPPAR2 to organotin compounds, we tested the relative expression level of CgPPAR2 after TPT injection by qRT-PCR. As illustrated in Fig. 2A, the expression of CgPPAR2 was up-regulated after TPT injection, indicating the activating effect of TPT exposure on this gene.

A phylogenetic analysis of NRs was conducted using 348 homologues including 47*C. gigas* NR proteins, of which two duplicated *C. gigas* NRs were simplified (Table S3). Four newly identified nuclear receptors are highlighted with asterisks in the maximum likelihood (ML) tree in File S4. Notably, CgPPAR2 groups with PPARs of some gastropods including *Biomphalaria glabrata*, *Lottia_gigantea* and *Patella depressa*, jointly belonging to a larger PPAR clade containing branches of vertebrate PPARα, PPARβ and PPARγ.

In terms of *CgBCOL* genes, within *CgBCOLb* and *CgBCOLc* group, similarities of protein and promoter sequences are very high (96.58% ~ 100%), so we analyze *CgBCOLb* and *CgBCOLc* group as one gene, respectively (table S4). Signal peptides and the functional domain (RPE65, accession number: pfam03055) of CgBCOL proteins are illustrated in Fig. 1 (A, B and C). Analysis of gene expression patterns showed that *CgBCOL* genes are mainly expressed in the digestive gland and hepatopancreas (Fig. S1). The ML tree showed that CgBCOL proteins belong to the large BCOL branch independent from metazoan BCO1 and BCO2 (File S5). Specifically, CgBCOLa grouped with *Mizuhopecten yessoensis* BCOL-7, while CgBCOLa and CgBCOLb group together and are closely related to *Mizuhopecten yessoensis* BCOL-1 to BCOL-6.

3.2. CgPPAR2 interacts with CgRXR at the protein level.

To test the protein–protein interaction between CgPPAR2 and CgRXR, we used a mammalian two-hybrid system and a yeast two-hybrid system to analyze the interaction between CgPPAR2 LBD and CgRXR LBD. In HEK293T cells, after co-transfection of recombinant plasmids, pBind-CgPPAR2 LBD and pACT-CgRXR LBD, to produce fusion proteins (CgPPAR2 LBD-GAL4 DBD, CgRXR LBD-VP16), the

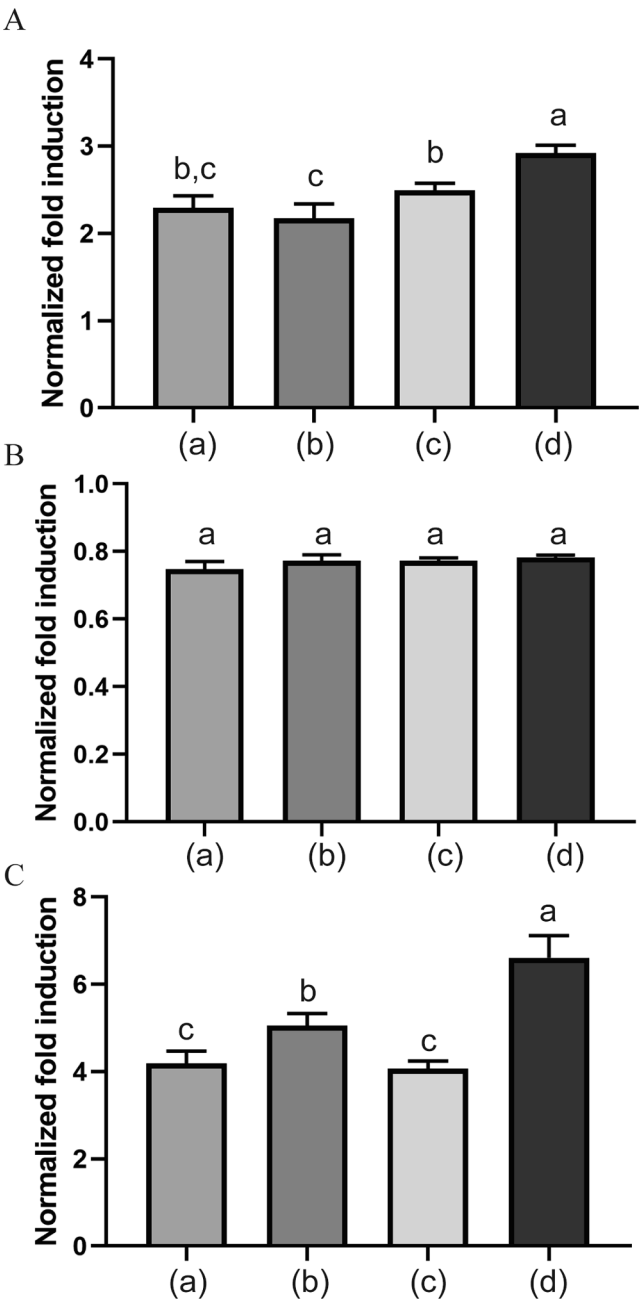

Fig. 3. The CgPPAR2/CgRXR heterodimer activates the transcription of *CgBCOLa* and *CgBCOLc*, but not *CgBCOLb*. Luciferase reporter vector fused with promoters of *CgBCOLa* (A), *CgBOCLb* (B) and *CgBCOLc* (C), as well as expression vectors for CgPPAR2 or CgRXR, singly or in combination were transfected into HEK293T cells. Cells transfected with empty pcDNA3.1 and empty pGL3-basic were used as empty group. The cells of negative control groups were transfected with empty pcDNA3.1 and Luciferase reporter vector fused with promoters. The total amount of DNA for each transfection was kept constant (550 ng) using empty pcDNA3.1. The ratio of Firefly luciferase and Renilla luciferase luminescence was normalized to the empty group. Technique replicates for each test condition and the entire experiment were performed at least twice. Results are presented as mean ± SD and a one-way ANOVA analysis. Columns marked with different letters were significantly different ($P < 0.05$). empty group: pcDNA3.1-empty, pGL3-Basic-empty, pRL-TK; (a) negative control group: pcDNA3.1-empty, pGL3-CgBCOL-a,b,c-Promoter, pRL-TK; (b) single CgPPAR2 group: pcDNA3.1-CgPPAR2, pcDNA3.1-empty, pGL3-CgBCOL-a,b,c-Promoter; (c) single CgRXR group: pcDNA3.1-CgRXR, pcDNA3.1-empty, pGL3-CgBCOL-a,b,c-Promoter, pRL-TK; (d) CgPPAR2/CgRXR heterodimer group: pcDNA3.1-CgPPAR2, pcDNA3.1-CgRXR, pGL3-CgBCOL-a,b,c-Promoter, pRL-TK.

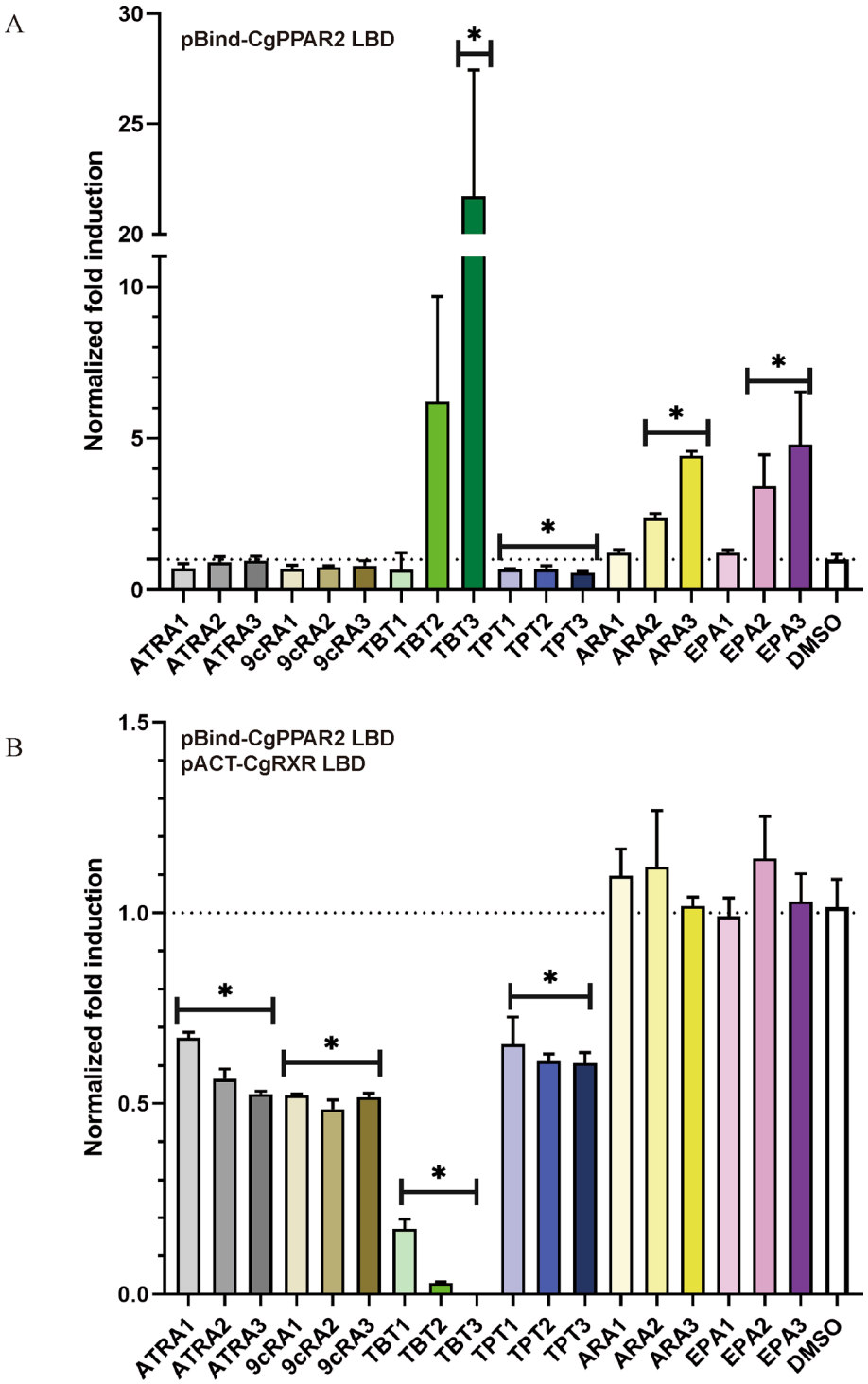

Fig. 4. Luciferase luminescence based on (A) transfection of pBind-CgPPAR2 LBD, and (B) co-transfection of pBind-CgPPAR2 LBD/pACT-CgRXRLBD in the presence of different concentrations of ligands. Values are presented as mean ± standard error (n = 3) of the normalized fold-induction (* $P < 0.05$). ATRA1-3, 9CRA1-3 (1 μM, 2 μM, 3 μM); TBT1-3, TPT1-3 (0.1 μM, 0.2 μM, 0.3 μM); ARA1-3, EPA1-3 (100 μM, 200 μM, 300 μM).

luminescence ratio of Firefly Luciferase (pGL4.31) and Renilla Luciferase (pBIND) significantly increased ($P < 0.0001$, Fig. 2B). In the Y2H yeast strain, yeast colonies co-transfected with PGBKT7-PPAR-LGD and PGADT7-RXR-LGD survived on the TDO medium with 5 mM 3′AT but not on the QDO medium (Fig. 2C). Both of the above experiments indicated that CgPPAR2 can physically interact with CgRXR.

3.3. The CgPPAR2/CgRXR heterodimer regulates CgBCOLa and CgBCOLc

To investigate whether the expression of *CgBCOL* genes can be regulated by the CgPPAR2/CgRXR heterodimer, we performed DLR assays using the pcDNA3.1/pGL3-Basic system in HEK293T cells. The results showed that co-transfection of pcDNA3.1 plasmids containing CDS of *CgPPAR2* and *CgRXR* significantly induced the expression of Firefly luciferase in reporter vectors fused with the promoters of

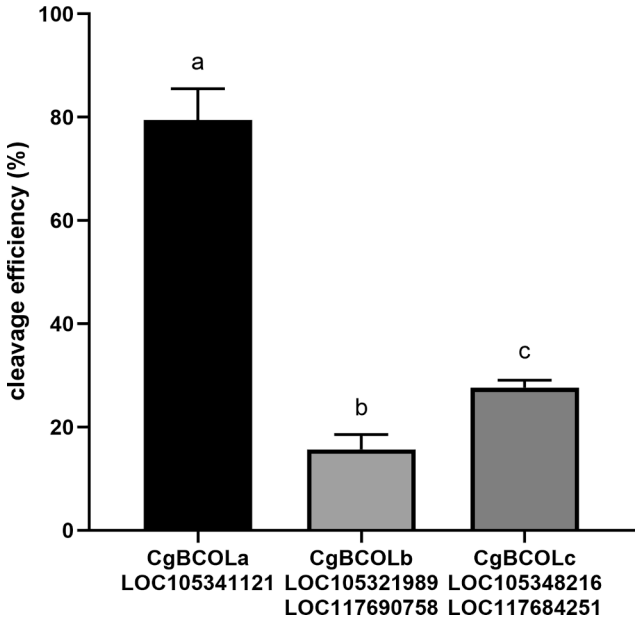

Fig. 5. comparison of beta-carotene cleavage efficiencies of CgBCOL. Columns marked with different letters were significantly different ($P < 0.05$).

CgBCOLa and *CgBCOLc* group, comparing with the control groups ($P < 0.001$). However, no significant difference was detected in the CgBCOLb group (Fig. 3). This indicated that CgPPAR2/CgRXR heterodimer can transactivate expressions of CgBCOLa and CgBCOLc, but not CgBCOLb. Besides, slight differences were present in the single NR transfected group (Fig. 3A, C), suggesting the slight effects of single NR on the transcription of *CgBCOLa* and *CgBCOLc*.

3.4. Effects of ligands on CgPPAR2 alone and the CgPPAR2/CgRXR heterodimer

The pBind/pACT DLR system was used in HEK293T cells exposed to natural and artificial chemicals to investigate the response of CgPPAR2 to ligands. This system could exclude the influence of DBD of target genes and examine the transactivation activity of LBD alone.

In cells transfected with pBind-CgPPAR2 LBD alone, as shown in Fig. 4A and Fig. S2, CgPPAR2 LBD could be activated by TBT, ARA, EPA in a dose-dependent manner. The highest fold induction was 28.3 at a concentration of 0.3 μM for TBT, as well as 4.6 and 6.7 at a concentration of 300 μM for ARA and EPA. However, transactivation of CgPPAR2 LBD was significantly inhibited by all three concentrations of TPT (0.1 μM, 0.2 μM, 0.3 μM), and was not affected by retinoid ligands, i.e., ATRA and 9cRA. As shown in Fig. 4B and Fig. S3, when cells co-transfected with pBind-CgPPAR2 LBD and pACT-CgRXR LBD were exposed to ligands, ATRA, 9cRA, TBT and TPT caused significant inhibition (more than half), among which the inhibition of ATRA and TBT shown a concentration-dependent manner.

3.5. Prokaryotic expression and beta-carotene cleavage efficiencies of CgBCOL genes

To validate the carotenoid cleavage function of *CgBCOL* genes, the signal peptide-removed coding sequences were subcloned into the expression vector pET-28a (+) to produce CgBCOL proteins. The obtained recombinant plasmid and the beta-carotene-producing plasmid were co-transformed into the JM109(DE3) *E. coli* strain, followed by SDS-PAGE that verified the presence of CgBCOL proteins (Fig. S4). Then the cleavage efficiencies were calculated based on the absorbance of supernatants at 480 nm and relative total number of bacterial cells. As shown in Fig. 5, beta-carotene cleavage efficiencies of *CgBCOL* genes significantly differ from each other, with a maximum of 85.16% (CgBCOLa) and a minimum of 12.54% (CgBCOLb).

3.6. Subcellular localization of CgPPAR2 protein

To investigate the subcellular localization of CgPPAR2 protein, recombinant plasmids producing GFP-tagged CgPPAR2 fusion protein were transferred into HEK293T cells, and cells transferred with the empty pEGFP-N1 plasmid without gene insertion were used as the control. As shown in Fig. 6, All the nuclei showed blue fluorescent signal. In cells transfected with empty pEGFP-N1, the green fluorescent signal was observed on cytoplasm, while in cells transfected with the CgPPAR2-GFP vector, the green fluorescent signal was detected in the nuclei. These results indicated that CgPPAR2 protein is localized in the

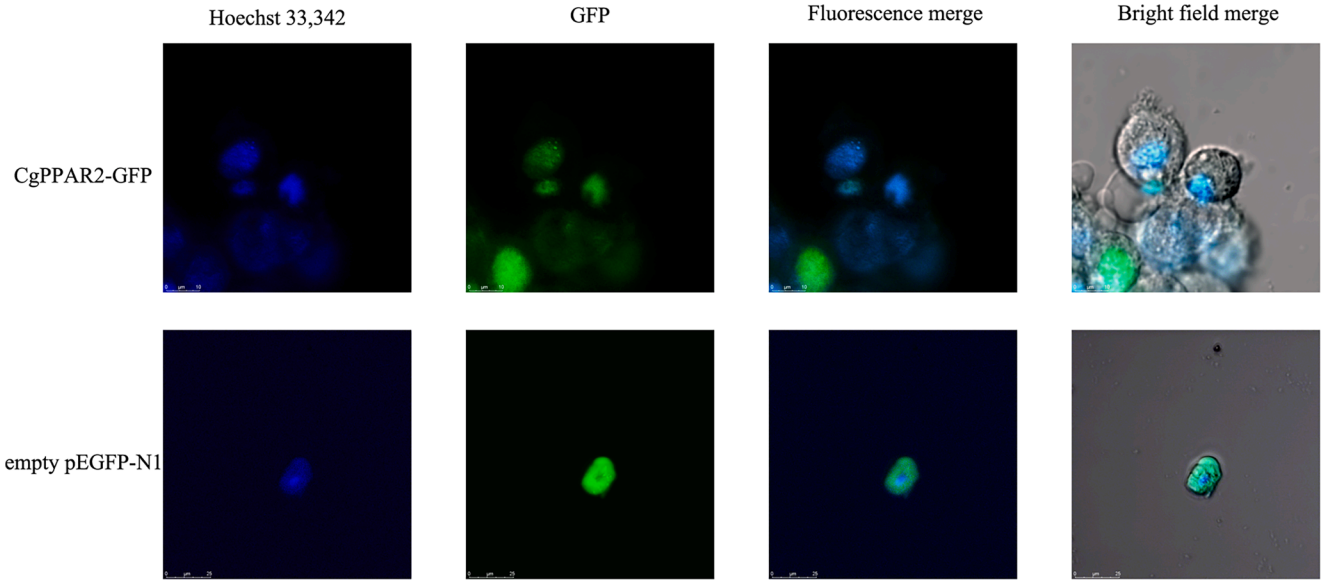

Fig. 6. Subcellular localization of CgPPAR2 in HEK293T cells. Cells were transfected with pEGFP-N1 fused with CgPPAR2 (top), and empty pEGFP-N1 (bottom), respectively. The blue fluorescent signal represents the nuclei and the green fluorescent signal represents the location of GFP protein. (For interpretation of the references to colour in this figure legend, the reader is referred to the web version of this article.)

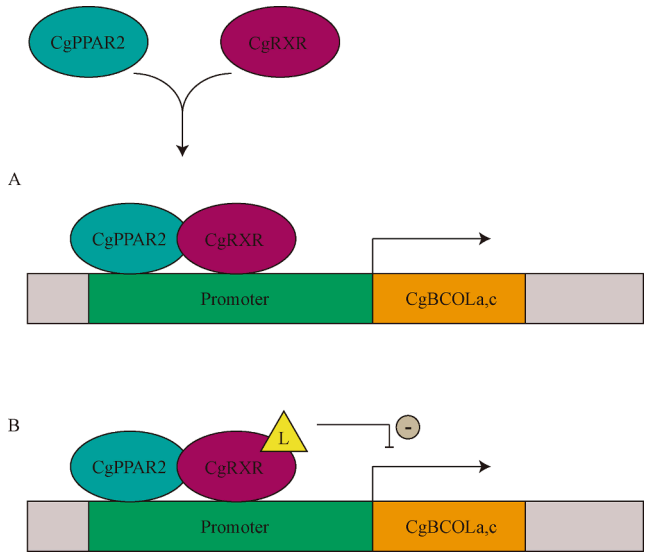

Fig. 7. Schematic representation of the putative mechanism for the regulation of *CgBCOLa* and *CgBCOLc* by the CgPPAR2/CgRXR heterodimer and ligands. CgPPAR2, peroxisome proliferator-activated receptor of *C. gigas*; CgRXR, retinoid X receptor of *C. gigas*; L, ligands including All-*trans*-RA (ATRA), 9-*cis*-RA (9cRA), tributyltin (TBT) and triphenyltin (TPT).

nuclei in HEK293T cells, supporting its characterization as a transcription factor.

4. Discussion

Peroxisome proliferator-activated receptor (*PPAR*) has been reported recently in several vertebrate and invertebrate species, highlighting their roles in regulating lipid metabolism and mediating endocrine disruption (Capitao et al., 2018; Capitao et al., 2020; Capitao et al., 2021). In the present study, in addition to *CgPPAR1* (Vogeler et al., 2014; Vogeler et al., 2017), we identified and characterized another *C. gigas PPAR* gene (*CgPPAR2*), which was hypothesized to be involved in carotenoid metabolism in our previous study (Wan et al., 2022). The CgPPAR2 protein sequence contains the typical conserved DBD and LBD domains of PPAR (Fig. 1D), as well as NLS validated by subcellular localization in HEK293T cells (Fig. 6). Importantly, our Maximum Likelihood phylogenetic analysis revealed that CgPPAR2 grouped with *P. depressa* PPAR2 (File S4) which has been reported as a direct orthologue of vertebrate PPARs by Capitao et al. (2021) using a phylogenetic and synteny analysis. Furthermore, given that PPARγ in vertebratetes has been reported to control BCO1 involved in carotenoid cleavage (Boulanger et al., 2003; Lietz et al., 2010), it is reasonable to speculate that CgPPAR2 may be a orthologue of vertebrate PPARs and play similar roles in *C. gigas*.

For nuclear receptors such as RAR, thyroid hormone receptor (TR) and PPAR, heterodimerization with the chaperone RXR is a typical feature necessary for their functions (Dawson and Xia, 2012). In *C. gigas*, Vogeler et al. (2017) predicted that CgPPAR1 could heterodimerize with CgRXR. Our observations on CgPPAR2 by DLR and two-hybrid assays suggested that CgPPAR2 is able to form heterodimer with CgRXR, which is consistent with reports in various metazoan lineages, such as mammals (Boulanger et al., 2003; Tyagi et al., 2011), teleosts (Barbosa et al., 2019), echinoderms (Capitao et al., 2020) and molluscs (Capitao et al., 2021), supporting the conservation of the PPAR/RXR heterodimers. In humans, PPARγ, RXRα, PPARγ/RXRα can increase the expression of the reporter gene fused with *BCO1* promoter in an additive manner (Gong et al., 2006), highlighting the importance of heterodimerization. This supports our finding that single CgPPAR2 or CgRXR has a slight effect on the *CgBCOLa* and *CgBCOLc* promoter activities, whereas CgPPAR2/CgRXR heterodimer can significantly transactivate the *CgBCOLa* and *CgBCOLc* promoters (Fig. 3; Fig. 7A). However, no significant differences were observed for the *CgBCOLb* promoter. This is consistent with our previous findings that dietary beta-carotene supplement resulted in down-regulation of *CgBCOLa* and *CgBCOLc*, but no change in *CgBCOLb* (Wan et al., 2022), indicating that there may be a different regulatory mechanism for *CgBCOLb*.

Tissue expression analyses using the RNA-Seq data from Zhang et al. (2012) and Xu et al. (2021) revealed that *CgBCOL* genes are mainly expressed in the digestive gland (including hepatopancreas) of *C. gigas* (Fig. S1), highlighting the importance of this organ as a main site for carotenoid metabolism, because it has been demonstrated by Xu et al. (2021) that there are functional similarities between the oyster and vertebrate digestive tissues, and the vertebrate liver and intestine are main sites for carotenoid metabolism (Raghuvanshi et al., 2015; Widjaja-Adhi et al., 2015). Meanwhile, the ubiquitous expression of *CgPPAR2* and *CgRXR* in various tissues, supporting their regulating *CgBCOL* genes in the digestive gland, and the fundamental role in lipid metabolism, energy supply (Morais, 2003) and signaling (Hessel et al., 2007) in all tissues. Notably, beta-carotene cleavage efficiencies of CgBCOL are significantly different from each other, revealing their distinct enzymatic properties. This functional difference may correspond to their different regulation by the CgPPAR2/CgRXR heterodimer.

A diet-responsive negative feedback regulatory mechanism in vertebrate intestine controlling carotenoid cleavage has been well described, which is regulated by intestine specific homeobox transcription factor (ISX) (Seino et al., 2008) and the RAR/RXR heterodimer capable of binding to retinoic acid (RA). Moreover. BCO1 can be regulated by ISX, and the PPARγ/RXR heterodimer (Lobo et al., 2010b). Similarly, in our previous study, we hypothesized the existence of a negative feedback regulatory network in *C. gigas*, in which nuclear receptor transcription factors may regulate carotenoid cleavage oxygenases (Wan et al., 2022). Here, our findings that CgPPAR2/CgRXR heterodimer transactivates of *CgBCOL* gene expression (Fig. 3) and this transactivation can be repressed by natural ligands, i.e., carotenoid cleavage derivatives (ATRA and 9cRA) (Fig. 4B; Fig. 7B; Fig. S3) verified this hypothesis. Specifically, *CgBCOL* essentially activated by CgPPAR2/CgRXR heterodimer can catalyze the cleavage of beta-carotene and promote the production of retinoid ligands including ATRA and 9cRA. Thus, when dietary supply of beta-carotene is adequate, the resulting excessive retinoids may inhibit the transactivation activity of the heterodimer, thereby down-regulating *CgBCOL* gene expression and retinoid production. Besides, we found that other natural ligands, i.e., fatty acids (ARA and EPA), can activate single CgPPAR2 (Fig. 4A; Fig. S2). This is consistent with the findings in mammals (Xu et al., 1999), chondrichthyan *Leucoraja erinacea* (Capitao et al., 2018), echinoderm *Paracentrotus lividus* (Capitao et al., 2020), and gastropod *Patella depressa* (Capitao et al., 2021), supporting the conservation of these ligands in vertebrates and invertebrates.

The organotins TBT and TPT are known environmental endocrine disruptors (Lima et al., 2011). PPAR/RXR has been shown to be regulated by these organotins that result in lipid homeostasis perturbation in species such as teleost fish *Pleuronectes platessa* (European plaice) (Colliar et al., 2011) and *P. depressa* (Capitao et al., 2021), as well as inhibit the activity of PPAR. Consistently, in the present study, single CgPPAR2 and CgPPAR2/CgRXR heterodimer are generally repressed by TBT and TPT, except that a high concentration of TBT (0.3 μM) greatly activated CgPPAR2 (Fig. 4; Fig. S2; Fig. S3). Furthermore, TPT injection induced the mRNA expression of *CgPPAR2* in the digestive glands (Fig. 2A). This result indicated that transcription of *CgPPAR2* can response to TPT exposure, suggesting the endocrine disruption of this organotin compound. Nevertheless, this activation of *CgPPAR2* expression did not mean that CgPPAR2 protein can interact with TPT. These results demonstrated that organotins can interact with CgPPAR2/CgRXR regulating carotenoid metabolism, providing a new prospect for

endocrine disruption by organotins in shellfish.

5. Conclusion

Taken together, we identified and characterized a novel *C. gigas PPAR* gene (*CgPPAR2*) as a nuclear receptor transcription factor. Functional assays showed that CgPPAR2 can form heterodimer with CgRXR, and then regulate carotenoid cleavage oxygenases by interacting with *CgBCOL* promoters and retinoid ligands in *C. gigas*. We demonstrated the existence of a negative feedback regulatory mechanism of carotenoid cleavage for retinoid production, which is controlled by the CgPPAR2/CgRXR heterodimer capable of binding to retinoids, and may be disrupted by organotins. Our findings on the *CgPPAR2* gene contribute to the understanding of the role of nuclear receptors, carotenoid metabolism and potential effects of organotins in mollusks.

CRediT authorship contribution statement

Sai Wan: Writing – original draft, Methodology. **Qi Li:** Supervision, Writing – review & editing. **Hong Yu:** Resources. **Shikai Liu:** Project administration. **Lingfeng Kong:** Resources.

Declaration of Competing Interest

The authors declare that they have no known competing financial interests or personal relationships that could have appeared to influence the work reported in this paper.

Acknowledgements

This study was supported by National Natural Science Foundation of China (31972789), the China Agriculture Research System Project (CARS-49), and Earmarked Fund for Agriculture Seed Improvement Project of Shandong Province (2020LZGC016).

Appendix A. Supplementary material

File S1. Protein sequences of nuclear receptors used in Phylogenetic analyses. The NCBI accession numbers were included in the sequence names.

File S2. Protein sequences of carotenoid cleavage oxygenases used in Phylogenetic analyses. The NCBI accession numbers were included in the sequence names.

File S3. conserved domain regions of the newly identified four receptors validated by Sanger sequencing.

File S4. The maximum likelihood phylogenetic tree of nuclear receptors.

File S5. The maximum likelihood phylogenetic tree of carotenoid cleavage oxygenases.

Table S1. Sequences, usage, restriction enzyme sites and target gene information of primers.

Table S2. Details on the use of plasmids and ligand compounds.

Table S3. Correspondence between the NRs identified by Vogeler et al. (2014) and the NRs identified in this work.

Table S4. protein and promoter sequence similarities of *CgBCOL* genes

Supplementary data to this article can be found online at https://doi.org/10.1016/j.gene.2022.146473.

References

Almagro Armenteros, J.J., Tsirigos, K.D., Sønderby, C.K., Petersen, T.N., Winther, O., Brunak, S., von Heijne, G., Nielsen, H., 2019. SignalP 5.0 improves signal peptide predictions using deep neural networks. Nat Biotechnol 37 (4), 420–423.

Amengual, J., Gouranton, E., van Helden, Y.G.J., Hessel, S., Ribot, J., Kramer, E., Kiec-Wilk, B., Razny, U., Lietz, G., Wyss, A., Dembinska-Kiec, A., Palou, A., Keijer, J., Landrier, J.F., Bonet, M.L., von Lintig, J., Srivastava, R.K., 2011. Beta-carotene reduces body adiposity of mice via BCMO1. PLoS ONE 6 (6), e20644.

Bachmann, H., Desbarats, A., Pattison, P., Sedgewick, M., Riss, G., Wyss, A., Cardinault, N., Duszka, C., Goralczyk, R., Grolier, P., 2002. Feedback regulation of beta, beta-carotene 15,15'-monooxygenase by retinoic acid in rats and chickens. J Nutr 132, 3616–3622.

Barbosa, M.A.G., Capela, R., Rodolfo, J., Fonseca, E., Montes, R., André, A., Capitão, A., Carvalho, A.P., Quintana, J.B., Castro, L.F.C., Santos, M.M., 2019. Linking chemical exposure to lipid homeostasis: A municipal waste water treatment plant influent is obesogenic for zebrafish larvae. Ecotoxicol Environ Saf 182, 109406.

Boulanger, A., McLemore, P., Copeland, N.G., Gilbert, D.J., Jenkins, N.A., Yu, S.S., Gentleman, S., Redmond, T.M., 2003. Identification of beta-carotene 15, 15'-monooxygenase as a peroxisome proliferator-activated receptor target gene. FASEB J 17 (10), 1304–1306.

Capitão, A., Lopes-Marques, M., Páscoa, I., Ruivo, R., Mendiratta, N., Fonseca, E., Castro, L.F.C., Santos, M.M., 2020. The Echinodermata PPAR: Functional characterization and exploitation by the model lipid homeostasis regulator tributyltin. Environ Pollut 263, 114467.

Capitão, A.M.F., Lopes-Marques, M., Páscoa, I., Sainath, S.B., Hiromori, Y., Matsumaru, D., Nakanishi, T., Ruivo, R., Santos, M.M., Castro, L.F.C., 2021. An ancestral nuclear receptor couple, PPAR-RXR, is exploited by organotins. Sci Total Environ 797, 149044.

Capitao, A.M.F., Lopes-Marques, M.S., Ishii, Y., Ruivo, R., Fonseca, E.S.S., Pascoa, I., Jorge, R.P., Barbosa, M.A.G., Hiromori, Y., Miyagi, T., Nakanishi, T., Santos, M.M., Castro, L.F.C., 2018. Evolutionary Exploitation of Vertebrate Peroxisome Proliferator-Activated Receptor gamma by Organotins. Environ Sci Technol 52, 13951–13959.

Casals-Casas, C., Feige, J.N., Desvergne, B., 2008. Interference of pollutants with PPARs: endocrine disruption meets metabolism. Int J Obes (Lond) 32 (Suppl 6), S53–S61.

Chen, S., Zhou, Y., Chen, Y., Gu, J., 2018. fastp: an ultra-fast all-in-one FASTQ preprocessor. Bioinformatics 34, i884–i890.

Colliar, L., Sturm, A., Leaver, M.J., 2011. Tributyltin is a potent inhibitor of piscine peroxisome proliferator-activated receptor alpha and beta. Comp Biochem Physiol C Toxicol Pharmacol 153, 168–173.

Cunningham Jr., F.X., Gantt, E., 2005. A study in scarlet: enzymes of ketocarotenoid biosynthesis in the flowers of Adonis aestivalis. Plant J 41, 478–492.

Cunningham, F.X., Gantt, E., 2007. A portfolio of plasmids for identification and analysis of carotenoid pathway enzymes: Adonis aestivalis as a case study. Photosynth Res 92 (2), 245–259.

Dawson, M.I., Xia, Z., 2012. The retinoid X receptors and their ligands. Biochim Biophys Acta 1821 (1), 21–56.

Diamanti-Kandarakis, E., Bourguignon, J.P., Giudice, L.C., Hauser, R., Prins, G.S., Soto, A.M., Zoeller, R.T., Gore, A.C., 2009. Endocrine-disrupting chemicals: an Endocrine Society scientific statement. Endocr Rev 30, 293–342.

Fitzpatrick, T.B., Basset, G.J.C., Borel, P., Carrari, F., DellaPenna, D., Fraser, P.D., Hellmann, H., Osorio, S., Rothan, C., Valpuesta, V., Caris-Veyrat, C., Fernie, A.R., 2012. Vitamin deficiencies in humans: can plant science help? Plant Cell 24 (2), 395–414.

Fonseca, E., Ruivo, R., Borges, D., Franco, J.N., Santos, M.M., Castro, L.F.C., 2020. Of Retinoids and Organotins: The Evolution of the Retinoid X Receptor in Metazoa. Biomolecules 10 (4), 594.

Giraud-Billoud, M., Castro-Vazquez, A., 2019. Aging and retinoid X receptor agonists on masculinization of female *Pomacea canaliculata*, with a critical appraisal of imposex evaluation in the Ampullariidae. Ecotoxicol Environ Saf 169, 573–582.

Gong, X., Tsai, S.W., Yan, B., Rubin, L.P., 2006. Cooperation between MEF2 and PPARgamma in human intestinal beta, beta-carotene 15,15'-monooxygenase gene expression. BMC Mol Biol 7, 7.

Harada, S., Hiromori, Y., Nakamura, S., Kawahara, K., Fukakusa, S., Maruno, T., Noda, M., Uchiyama, S., Fukui, K., Nishikawa, J., Nagase, H., Kobayashi, Y., Yoshida, T., Ohkubo, T., Nakanishi, T., 2015. Structural basis for PPARgamma transactivation by endocrine-disrupting organotin compounds. Sci Rep 5, 8520.

Hessel, S., Eichinger, A., Isken, A., Amengual, J., Hunzelmann, S., Hoeller, U., Elste, V., Hunziker, W., Goralczyk, R., Oberhauser, V., von Lintig, J., Wyss, A., 2007. CMO1 deficiency abolishes vitamin A production from beta-carotene and alters lipid metabolism in mice. J Biol Chem 282, 33553–33561.

Huang, W., Wu, Q., Xu, F., Li, L.i., Li, J., Que, H., Zhang, G., 2020. Functional characterization of retinoid X receptor with an emphasis on the mediation of organotin poisoning in the Pacific oyster (Crassostrea gigas). Gene 753, 144780.

Jin, K., Jin, Q., Cai, Z., Huang, B., Wei, L., Zhang, M., Guo, W., Liu, Y., Wang, X., 2021. Molecular Characterization of Retinoic Acid Receptor CgRAR in Pacific Oyster (Crassostrea gigas). Front Physiol 12, 666842.

Katoh, K., Misawa, K., Kuma, K., Miyata, T., 2002. MAFFT: a novel method for rapid multiple sequence alignment based on fast Fourier transform. Nucleic Acids Res 30, 3059–3066.

Kaur, S., Jobling, S., Jones, C.S., Noble, L.R., Routledge, E.J., Lockyer, A.E., Fong, P.P., 2015. The nuclear receptors of Biomphalaria glabrata and Lottia gigantea: implications for developing new model organisms. PLoS ONE 10 (4), e0121259.

Kuhn, D.D., Angier, M.W., Barbour, S.L., Smith, S.A., Flick, G.J., 2013. Culture feasibility of eastern oysters (Crassostrea virginica) in zero-water exchange recirculating aquaculture systems using synthetically derived seawater and live feeds. Aquacult. Eng. 54, 45–48.

Laudet, V., 2006. Nuclear Receptor Genes. John Wiley & Sons Ltd.

Lietz, G., Lange, J., Rimbach, G., 2010. Molecular and dietary regulation of beta, beta-carotene 15,15'-monooxygenase 1 (BCMO1). Arch Biochem Biophys 502, 8–16.

Lima, D., Reis-Henriques, M.A., Silva, R., Santos, A.I., Castro, L.F., Santos, M.M., 2011. Tributyltin-induced imposex in marine gastropods involves tissue-specific modulation of the retinoid X receptor. Aquat Toxicol 101, 221–227.
Lin, J.R., Mondal, A.M., Liu, R., Hu, J., 2012. Minimalist ensemble algorithms for genome-wide protein localization prediction. BMC Bioinf. 13, 157.
Lobo, G.P., Amengual, J., Li, H.N., Golczak, M., Bonet, M.L., Palczewski, K., von Lintig, J., 2010a. Beta, beta-carotene decreases peroxisome proliferator receptor gamma activity and reduces lipid storage capacity of adipocytes in a beta, beta-carotene oxygenase 1-dependent manner. J Biol Chem 285, 27891–27899.
Lobo, G.P., Hessel, S., Eichinger, A., Noy, N., Moise, A.R., Wyss, A., Palczewski, K., von Lintig, J., 2010b. ISX is a retinoic acid-sensitive gatekeeper that controls intestinal beta, beta-carotene absorption and vitamin A production. FASEB J 24, 1656–1666.
Lyssimachou, A., Navarro, J.C., Bachmann, J., Porte, C., 2009. Triphenyltin alters lipid homeostasis in females of the ramshorn snail Marisa cornuarietis. Environ Pollut 157 (5), 1714–1720.
Mangelsdorf, D.J., Thummel, C., Beato, M., Herrlich, P., Schütz, G., Umesono, K., Blumberg, B., Kastner, P., Mark, M., Chambon, P., Evans, R.M., 1995. The nuclear receptor superfamily: The second decade. Cell 83 (6), 835–839.
Maoka, T., 2011. Carotenoids in marine animals. Mar Drugs 9, 278–293.
Marchler-Bauer, A., Lu, S., Anderson, J.B., Chitsaz, F., Derbyshire, M.K., DeWeese-Scott, C., Fong, J.H., Geer, L.Y., Geer, R.C., Gonzales, N.R., Gwadz, M., Hurwitz, D.I., Jackson, J.D., Ke, Z., Lanczycki, C.J., Lu, F., Marchler, G.H., Mullokandov, M., Omelchenko, M.V., Robertson, C.L., Song, J.S., Thanki, N., Yamashita, R.A., Zhang, D., Zhang, N., Zheng, C., Bryant, S.H., 2011. CDD: a Conserved Domain Database for the functional annotation of proteins. Nucleic Acids Res 39 (Database), D225–D229.
Minh, B.Q., Nguyen, M.A.T., von Haeseler, A., 2013. Ultrafast approximation for phylogenetic bootstrap. Mol Biol Evol 30 (5), 1188–1195.
Morais, S., 2003. Gonad development and fatty acid composition of Patella depressa Pennant (Gastropoda: Prosobranchia) populations with different patterns of spatial distribution, in exposed and sheltered sites. J. Exp. Mar. Biol. Ecol. 294 (1), 61–80.
Novac, N., Heinzel, T., 2004. Nuclear receptors: overview and classification. Curr Drug Targets Inflamm Allergy 3, 335–346.
Ouadah-Boussouf, N., Babin, P.J., 2016. Pharmacological evaluation of the mechanisms involved in increased adiposity in zebrafish triggered by the environmental contaminant tributyltin. Toxicol Appl Pharmacol 294, 32–42.
Pascoal, S., Carvalho, G., Vasieva, O., Hughes, R., Cossins, A., Fang, Y., Ashelford, K., Olohan, L., Barroso, C., Mendo, S., Creer, S., 2013. Transcriptomics and in vivo tests reveal novel mechanisms underlying endocrine disruption in an ecological sentinel, Nucella lapillus. Mol Ecol 22 (6), 1589–1608.
Pertea, M., Pertea, G.M., Antonescu, C.M., Chang, T.-C., Mendell, J.T., Salzberg, S.L., 2015. StringTie enables improved reconstruction of a transcriptome from RNA-seq reads. Nat Biotechnol 33 (3), 290–295.
Poliakov, E., Soucy, J., Gentleman, S., Rogozin, I.B., Redmond, T.M., 2017. Phylogenetic analysis of the metazoan carotenoid oxygenase superfamily: a new ancestral gene assemblage of BCO-like (BCOL) proteins. Sci Rep 7, 13192.
Raghuvanshi, S., Reed, V., Blaner, W.S., Harrison, E.H., 2015. Cellular localization of beta-carotene 15,15' oxygenase-1 (BCO1) and beta-carotene 9',10' oxygenase-2 (BCO2) in rat liver and intestine. Arch Biochem Biophys 572, 19–27.
Renault, T., Faury, N., Barbosa-Solomieu, V., Moreau, K., 2011. Suppression substractive hybridisation (SSH) and real time PCR reveal differential gene expression in the Pacific cupped oyster, Crassostrea gigas, challenged with Ostreid herpesvirus 1. Dev Comp Immunol 35 (7), 725–735.
Santos, M.M., Ruivo, R., Capitao, A., Fonseca, E., Castro, L.F.C., 2018. Identifying the gaps: Resources and perspectives on the use of nuclear receptor based-assays to improve hazard assessment of emerging contaminants. J Hazard Mater 358, 508–511.
Seino, Y., Miki, T., Kiyonari, H., Abe, T., Fujimoto, W., Kimura, K., Takeuchi, A., Takahashi, Y., Oiso, Y., Iwanaga, T., Seino, S., 2008. Isx participates in the maintenance of vitamin A metabolism by regulation of beta-carotene 15,15'-monooxygenase (Bcmo1) expression. J Biol Chem 283, 4905–4911.
Takaichi, S., 2011. Carotenoids in algae: distributions, biosyntheses and functions. Mar Drugs 9, 1101–1118.
Tan, K., Guo, Z., Zhang, H., Ma, H., Li, S., Zheng, H., 2021. Carotenoids regulation in polymorphic noble scallops Chlamys nobilis under different light cycle. Aquaculture 531, 735937.
Tyagi, S., Gupta, P., Saini, A.S., Kaushal, C., Sharma, S., 2011. The peroxisome proliferator-activated receptor: A family of nuclear receptors role in various diseases. J Adv Pharm Technol Res 2, 236–240.
Vitting-Seerup, K., Sandelin, A., Berger, B., 2019. IsoformSwitchAnalyzeR: analysis of changes in genome-wide patterns of alternative splicing and its functional consequences. Bioinformatics 35 (21), 4469–4471.
Vogeler, S., Galloway, T.S., Isupov, M., Bean, T.P., Schubert, M., 2017. Cloning retinoid and peroxisome proliferator-activated nuclear receptors of the Pacific oyster and in silico binding to environmental chemicals. PLoS ONE 12 (4), e0176024.
Vogeler, S., Galloway, T.S., Lyons, B.P., Bean, T.P., 2014. The nuclear receptor gene family in the Pacific oyster, Crassostrea gigas, contains a novel subfamily group. BMC Genomics 15, 369.
Wan, S., Li, Q.i., Yu, H., Liu, S., Kong, L., 2022. Transcriptome analysis based on dietary beta-carotene supplement reveals genes potentially involved in carotenoid metabolism in Crassostrea gigas. Gene 818, 146226.
Widjaja-Adhi, M.A.K., Lobo, G.P., Golczak, M., Von Lintig, J., 2015. A genetic dissection of intestinal fat-soluble vitamin and carotenoid absorption. Hum Mol Genet 24 (11), 3206–3219.
Xu, F., Marletaz, F., Gavriouchkina, D., Liu, X., Sauka-Spengler, T., Zhang, G., Holland, P. W.H., 2021. Evidence from oyster suggests an ancient role for Pdx in regulating insulin gene expression in animals. Nat Commun 12, 3117.
Xu, H.E., Lambert, M.H., Montana, V.G., Parks, D.J., Blanchard, S.G., Brown, P.J., Sternbach, D.D., Lehmann, J.M., Wisely, G.B., Willson, T.M., Kliewer, S.A., Milburn, M.V., 1999. Molecular Recognition of Fatty Acids by Peroxisome Proliferator-Activated Receptors. Mol. Cell 3 (3), 397–403.
Ye, J., Coulouris, G., Zaretskaya, I., Cutcutache, I., Rozen, S., Madden, T.L., 2012. Primer-BLAST: a tool to design target-specific primers for polymerase chain reaction. BMC Bioinf. 13, 134.
Zhang, G., Fang, X., Guo, X., Li, L.i., Luo, R., Xu, F., Yang, P., Zhang, L., Wang, X., Qi, H., Xiong, Z., Que, H., Xie, Y., Holland, P.W.H., Paps, J., Zhu, Y., Wu, F., Chen, Y., Wang, J., Peng, C., Meng, J., Yang, L., Liu, J., Wen, B.o., Zhang, N.a., Huang, Z., Zhu, Q., Feng, Y., Mount, A., Hedgecock, D., Xu, Z., Liu, Y., Domazet-Lošo, T., Du, Y., Sun, X., Zhang, S., Liu, B., Cheng, P., Jiang, X., Li, J., Fan, D., Wang, W., Fu, W., Wang, T., Wang, B.o., Zhang, J., Peng, Z., Li, Y., Li, N.a., Wang, J., Chen, M., He, Y., Tan, F., Song, X., Zheng, Q., Huang, R., Yang, H., Du, X., Chen, L.i., Yang, M., Gaffney, P.M., Wang, S., Luo, L., She, Z., Ming, Y., Huang, W., Zhang, S., Huang, B., Zhang, Y., Qu, T., Ni, P., Miao, G., Wang, J., Wang, Q., Steinberg, C.E.W., Wang, H., Li, N., Qian, L., Zhang, G., Li, Y., Yang, H., Liu, X., Wang, J., Yin, Y.e., Wang, J., 2012. The oyster genome reveals stress adaptation and complexity of shell formation. Nature 490 (7418), 49–54.
Zhao, S., Fernald, R.D., 2005. Comprehensive algorithm for quantitative real-time polymerase chain reaction. J Comput Biol 12 (8), 1047–1064.